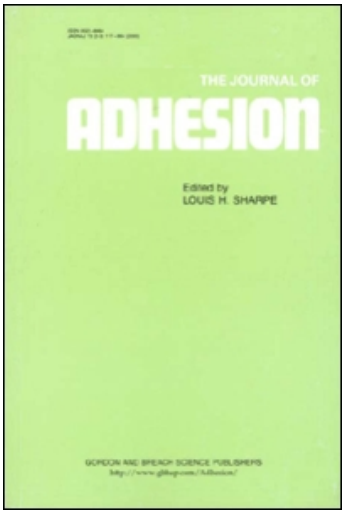

The Journal of Adhesion
Publication details, including instructions for authors and subscription information:
http://www.informaworld.com/smpp/title~content=t713453635

Plasma Surface Treatment of Aerospace Materials for Enhanced Adhesive Bonding

W. Leahy[a]; V. Barron[b]; M. Buggy[a]; T. Young[a]; A. Mas[c]; F. Schue[c]; T. McCabe[d]; M. Bridge[d]
[a] Materials and Surface Science Institute, University of Limerick, Limerick, Ireland [b] Department of Physics, Trinity College Dublin, Dublin, Ireland [c] Laboratoire de Chimie Macromoleculaire, Universite de Montpellier II, France [d] Dept. of Chemistry, Trinity College Dublin, Dublin, Ireland

To cite this Article Leahy, W. , Barron, V. , Buggy, M. , Young, T. , Mas, A. , Schue, F. , McCabe, T. and Bridge, M.(2001) 'Plasma Surface Treatment of Aerospace Materials for Enhanced Adhesive Bonding', The Journal of Adhesion, 77: 3, 215 — 249
To link to this Article: DOI: 10.1080/00218460108030739
URL: http://dx.doi.org/10.1080/00218460108030739

The Journal of Adhesion, 77: 215–249, 2001

0021-8464/01 $12.00 + .00

Plasma Surface Treatment of Aerospace Materials for Enhanced Adhesive Bonding

W. LEAHY[a], V. BARRON[b], M. BUGGY[a], T. YOUNG[a], A. MAS[c], F. SCHUE[c], T. McCABE[d], and M. BRIDGE[d]

[a]*Materials and Surface Science Institute, University of Limerick, Limerick, Ireland;* [b]*Department of Physics, Trinity College Dublin, Dublin, Ireland;* [c]*Laboratoire de Chimie Macromoleculaire, Universite de Montpellier II, Sciences et Techniques du Langeudoc, France;* [d]*Dept. of Chemistry, Trinity College Dublin, Dublin 2, Ireland*

(Received 9 November 2000; in final form 10 August 2001)

The increased use of polyphenylene sulphide (PPS) and polyetheretherketone based composites for aircraft structures has highlighted the need for reliable methods of bonding these materials to metallic components such as titanium. Both composite and titanium adhesive bonds exhibit poor long-term durability when exposed to hot/wet conditions, aerospace fluids and solvents. As a result, surface treatments are employed to enhance surface energy, surface roughness and alter surface chemistry to provide better long-term durability. In this initial study the adhesive bonding of glass fibre reinforced GFR-PPS and commercially pure titanium was investigated. Prior to bonding, both materials were plasma treated using argon and oxygen gases in a RF discharge. Surface characterisation was carried out to optimise these treatments. Surface energy and wettability were examined using contact angle analysis, surface roughness was examined using scanning electron microscopy and atomic force microscopy, while X-ray photoelectron spectroscopy (XPS) was employed to study the surface chemistry. Bond strengths were determined using lap shear tests. Initial results reveal that these optimum plasma treatments produce a significant increase in bond strength.

Keywords: Plasma treatment; Adhesive bonding; Aerospace materials; Titanium; Composites

Address correspondence to V. Barron, Department of Physics, Trinity College Dublin, Dublin 2, Ireland. E-mail: barronv@tcd.ie

INTRODUCTION

In this study, plasma surface treatment was employed to improve the bond strength of an adhesive joint of a glass-fibre-reinforced polyphenylene sulphide composite (GFR-PPS) and commercially pure titanium for an aerospace application. Previous researchers have shown plasma treatment to be an effective method of surface modification for enhancing bond strengths of polymer composite materials [1, 2, 3].

By relating the water contact angle of untreated GFR-PPS and titanium to plasma treated surfaces the optimum treatment was developed. In previous studies by Ameen [4] and Barron [5] it was found that the water contact angle increased with increase in storage time. This change in surface behaviour is believed to be due to rotation of surface polar groups, migration of low molecular weight fragments to the bulk or the release of low molecular weight oxidised material [5–9]. It has been suggested by Brennan *et al.* [6] that polymer surfaces can adapt to surrounding media by reorientation of the surface segments and such segments can produces changes in contact angle measurements. As a result of previous research carried out by Barron [5], this study investigated the change in water and methylene iodide contact angles with increasing storage time and temperature to determine the optimum plasma treatment conditions for bonding.

MATERIALS

Polyphenylene sulphide (PPS) is a semi crystalline material that offers an excellent balance of high temperature resistance, chemical resistance, dimensional stability and electrical properties. PPS is prepared using 1,4 dichlorobenzene and sodium sulphide in a polar solvent as shown in Figure 1.

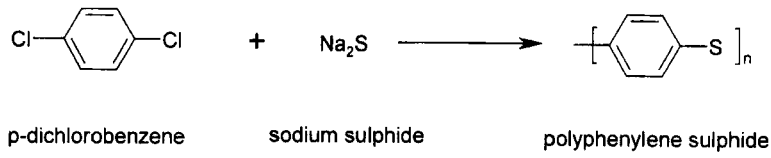

FIGURE 1 Chemical reaction for GFR-PPS.

PPS typically has a heat deflection temperature of over 260°C and a melting temperature of 285°C. In addition, PPS can survive an aggressive chemical environment. No solvents below 205°C are known to dissolve it and, unlike other aircraft materials such as polyetherimide, PPS does not absorb water [10]. The GFR-PPS composite used in this research was composed of a quasi-isotropic, 13-ply Glass/PPS laminate. The titanium used was a commercially pure (cp) grade, while the adhesive used was an epoxy-based FM 300-2 supplied by Cytec Engineering Materials Inc., USA. This new adhesive film, reported by Kohli [11] for aerospace bonding applications, is a 121°C cure version of the traditional 177°C cure FM-300 adhesive film which provides stress-strain and mechanical performance similar to the FM-300 system.

EXPERIMENTAL PROCEDURE

The surface of the GFR-PPS was degreased using acetone, then rinsed and cleaned ultrasonically in a bath of distilled water at 50°C for 1 hour. Finally, the samples were dried in vacuum oven at 60°C for 12 hours. The experimental set-up used for the plasma treatments is schematically illustrated in Figure 2.

The glow discharge was generated using a 13.56 MHz radio frequency generator. The energy was coupled to a pair of parallel aluminium electrodes, which are situated in a closed reactor. Prior to treatment, the chamber was cleaned thoroughly with ethanol and dried. The cleaned and degreased samples of approximately 2.5 cm × 1 cm × 0.3 cm were placed in the chamber on the bottom electrode. The chamber was then evacuated and the pressure stabilised at 4 Pa. The gas to be used for the plasma treatment was then introduced into the chamber. The flow rate of the gas was adjusted so that the pressure in the chamber was stabilised at 40 Pa for the plasma treatment process. The radio frequency (RF) was switched on and increased to the desired level, making sure that the reflected power was minimised. The samples were treated for the desired period of time and the RF was turned off, after which the chamber was then neutralised by allowing the gas to flow for another 15 minutes. It was then evacuated for 60 minutes. After treatment the samples were stored in sealed plastic containers at minus 16°C and at room temperature and in a fan oven at 125°C. Plasma treatments were carried out

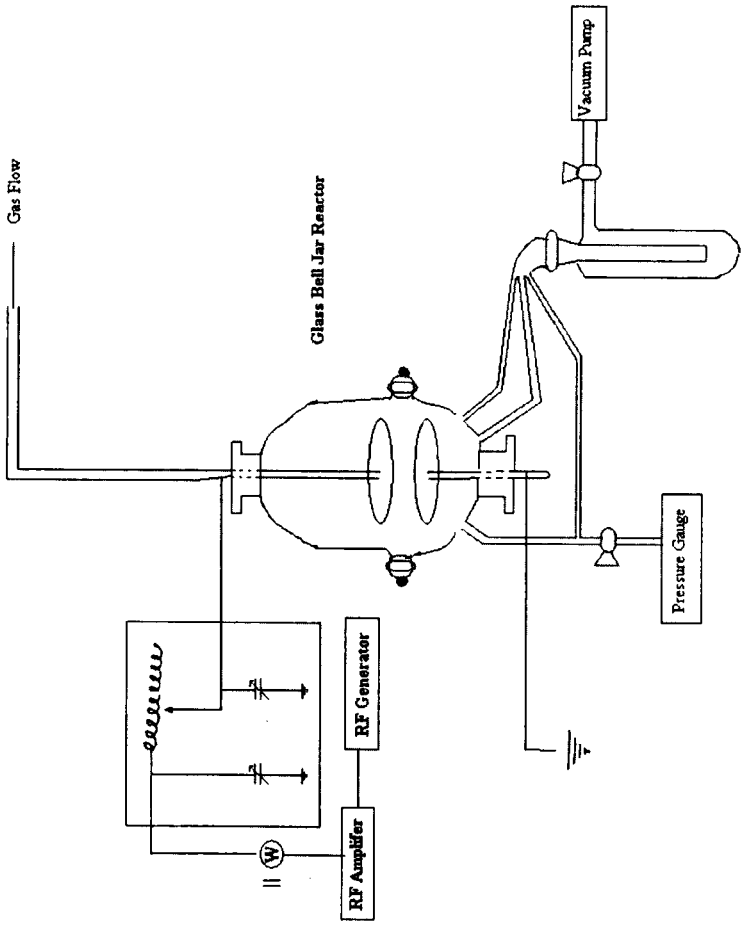

FIGURE 2 Schematic diagram of plasma treatment equipment.

using oxygen and argon gases and with various different operating conditions to optimise the treatment.

The adhesive joint was constructed as shown in Figure 3 and bonding was completed using a compression-moulding machine as follows.

To cure the system the assembly was

1. Heated to 120°C in 30 minutes
2. Held for 90 minutes at a pressure of 10 MPa
3. Cooled to room temperature at 5°C per minute.

Contact angles using water and methylene iodide were measured using the sessile drop technique on a KRUSS Model G23 Contact Angle Instrument. The temperature in the room was controlled and noted as 25°C. An average of 5 measurements were taken to avoid evaporation or absorption errors. The error of the measurement was taken as ±3° for each liquid. After treatment the contact angles were monitored after 2 hours, 1 day, 3 days, 7 days, 14 days and 30 days at −16°C, 25°C and 125°C in the three controlled environments discussed previously. Surface energies were determined from the water and methylene iodide contact angles using the following equations:

$$\gamma_s = \gamma_s^p + \gamma_s^d \tag{1}$$

where γ_s^p = polar component, γ_s^d = dispersive component. γ_s^d and γ_s^p are obtained by forming simultaneous equations from the following equation.

$$1 + \cos\theta = \frac{2(\gamma_s^{\mathrm{d}})^{1/2}(\gamma_{1v}^{\mathrm{d}})^{1/2}}{\gamma_v} + \frac{2(\gamma_s^{\mathrm{p}})^{1/2}(\gamma_{1v}^{\mathrm{p}})^{1/2}}{\gamma_{1v}} \tag{2}$$

The dispersion component is calculated as follows:

$$\gamma_s^d = \frac{(1+\cos\theta)^2}{4} \cdot \gamma_{1v} \tag{3}$$

where γ_{1v} = surface free energy of methylene iodide (50.8 mJm^{-2}).

The polar component is calculated as follows:

$$\gamma_s^p = \frac{1}{\gamma_{1v}^{\mathrm{p}}}\left[\frac{(1+\cos\theta)\cdot\gamma_{1v} - 2\sqrt{(\gamma_{1v}^{\mathrm{d}}\cdot\gamma_s^{\mathrm{d}})}}{2}\right]^2 \tag{4}$$

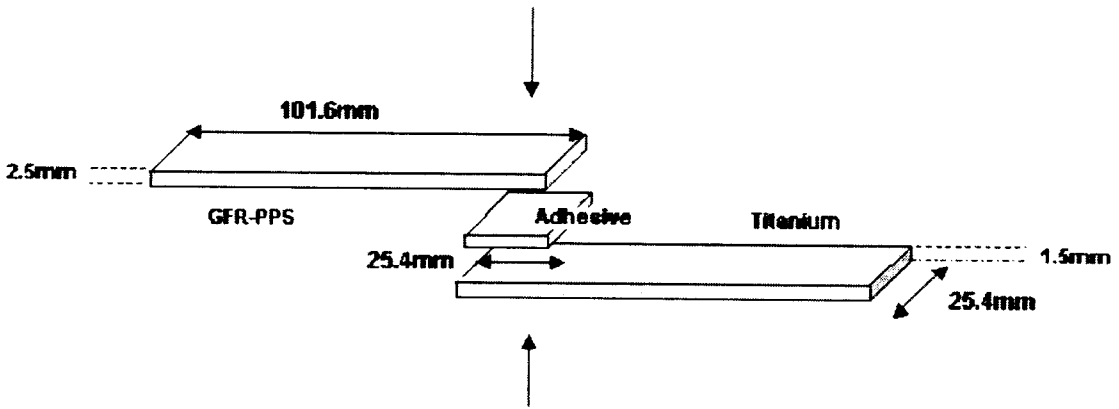

FIGURE 3 Lap shear joint configuration.

where γ_{lv}^{p} = polar component of the water, 51 mJm^{-2}, γ_{lv} is the surface free energy of water, 72.3 mJm^{-2}, and γ_{lv}^{d} = dispersion component of the water, 21.3 mJm^{-2}, and γ_{s}^{d} is the dispersion component of the substrate as calculated from Equation (3).

Surface topography was examined before and after treatment using SEM and AFM. Surface roughness was examined visually using a JEOL 6300F scanning electron microscope and quantitatively using a Topometrix TMX 2000 atomic force microscope, while the surface chemistry of the specimens was studied on a Vacuum Science Workshop Twin Anode ESCA Spectrometer. The bond strengths of adhesively bonded GFR-PPS/titanium joints were determined using single lap shear tests according to the standard ASTM D 5868-95.

RESULTS AND DISCUSSION

Contact Angle Analysis

Argon Plasma Treatment of GFR-PPS

The optimum treatment conditions for the plasma treatment of GFR-PPS were taken as those that produced the lowest water contact angle value after treatment. For the argon plasma treatment the lowest water contact angle values were found with a power of 100 W, pressure of 4O Pa and time of 30 minutes. The water contact angle for degreased GFR-PPS was 75°. Directly after treatment the contact angle had dropped to 8°. However, the modification was not stable. The effect of storage time and temperature on the contact angle values of argon plasma treated GFR-PPS are given in Table I. Two hours after treatment this value had increased to 23°, 36° and 65° for samples stored at −16°C, 25°C and 125°C, respectively. Storage temperature has a major effect on the rate of change of water contact angle. Samples stored at −16°C were the most stable, only increasing by 2–3° to 26° even a month after treatment. Samples stored at 25°C were only slightly less stable; the contact angle had increased by 10° to 46° one month after treatment. The largest change was observed in samples stored at 125°C. After only a day the contact angle had risen to 78°, which is higher than for the degreased sample.

TABLE I Contact angle values for argon plasma treated GFR-PPS. Degreased $\theta_{H_2O} = 75°$, $\theta_{CH_2I_2} = 51°$, directly alter treatment: $\theta_{H_2O} = 8°$, $\theta_{CH_2I_2} = 25°$

Storage Temp. (°C)						
Time after	−16		25		125	
treatment (hrs)	θ_{H_2O}(°)	$\theta_{CH_2I_2}$(°)	θ_{H_2O}(°)	$\theta_{CH_2I_2}$(°)	θ_{H_2O}(°)	$\theta_{CH_2I_2}$(°)
2	23	28	36	20	65	33
24	32	37	38	28	78	17
72	25	28	35	28	87	28
168	25	35	26	24	75	38
336	18	32	39	39	83	41
672	26	46	46	44	78	45

Oxygen Plasma Treatment of GFR-PPS

The lowest water contact angle values for oxygen plasma treatment were found using a power of 100 W and pressure of 40 Pa for 10 minutes. Table II shows the effect of storage time and temperature on the contact angle values of oxygen plasma treated GFR-PPS. It is interesting to note that the same initial water contact angle value as that for the argon plasma treated GFR-PPS (8°) was recorded directly after treatment. However, as shown in Table II, the oxygen treatment was slightly more stable than the argon treatment especially at 25°C where the contact angle had increased by only 4° one month after treatment. Overall, the trend was the same for both treatments. The lower storage temperature resulted in the lowest contact angle values. The most obvious difference between these two treatments is the effect of the treatment on the non-polar methylene iodide contact angle values. For argon plasma treatment there is an initial drop in the non-

TABLE II Contact angle values for oxygen plasma treated GFR-PPS. Degreased $\theta_{H_2O} = 75°$, $\theta_{CH_2I_2} = 51°$, directly after treatment: $\theta_{H_2O} = 8°$, $\theta_{CH_2I_2} = 27°$

Storage Temp. (°C)						
Time after	−16		25		125	
treatment (hrs)	θ_{H_2O}(°)	$\theta_{CH_2I_2}$(°)	θ_{H_2O}(°)	$\theta_{CH_2I_2}$(°)	θ_{H_2O}(°)	$\theta_{CH_2I_2}$(°)
2	22	46	29	44	51	46
24	24	45	31	42	55	46
72	27	45	30	44	67	49
168	29	44	29	43	82	40
672	27	45	33	48	86	44

polar contact angle to 25° immediately after treatment. However, after one month this value increases to 46°, which is just a few degrees below the value recorded for degreased GFR-PPS, suggesting that the effect of surface groups are being lost either by migration of these groups to the bulk of the material as suggested by Brennan *et al.* [6] or, as Foerch *et al.* [12] state, by chain motion as the surface attempts to stabilize itself after plasma exposure. In the case of the oxygen plasma treatment this increase in the methylene iodide contact angle occurs much faster. After 2 hours the value had increased to 46°, 44° and 46° for samples stored at −16°C, 25°C and 125°C, respectively. This could also be due to the release of low molecular oxidized materials as suggested by Strobel *et al.* [8].

Plasma Treatment of Titanium

Contact angle values for the argon plasma treated titanium are given in Table III, while oxygen plasma treatment results are shown in Table IV. Optimum treatments were found to be 30 and 10 minutes at a

TABLE III Contact angle values for argon plasma treated titanium. Degreased $\theta_{H_2O} = 83°$, $\theta_{CH_2I_2} = 55°$, directly after treatment: $\theta_{H_2O} = 13°$, $\theta_{CH_2I_2} = 38°$

Temp. (°C)	−16		25		125	
Time after treatment (hrs)	θ_{H_2O}(°)	$\theta_{CH_2I_2}$(°)	θ_{H_2O}(°)	$\theta_{CH_2I_2}$(°)	θ_{H_2O}(°)	$\theta_{CH_2I_2}$(°)
2	25	42	27	41	40	42
24	8	43	31	53	54	41
72	35	42	30	47	54	39
168	31	42	58	45	58	42
672	14	45	70	46	52	48

TABLE IV Contact angle values for oxygen plasma treated titanium. Degreased $\theta_{H_2O} = 83°$, $\theta_{CH_2I_2} = 55°$, directly after treatment: $\theta_{H_2O} = 10°$, $\theta_{CH_2I_2} = 38°$

Temp. (°C)	−16		25		125	
Time after treatment (hrs)	θ_{H_2O}(°)	$\theta_{CH_2I_2}$(°)	θ_{H_2O}(°)	$\theta_{CH_2I_2}$(°)	θ_{H_2O}(°)	$\theta_{CH_2I_2}$(°)
2	20	46	37	45	55	38
24	33	46	33	45	47	48
72	17	59	39	46	48	49
168	30	46	60	43	61	45
672	34	44	69	46	65	48

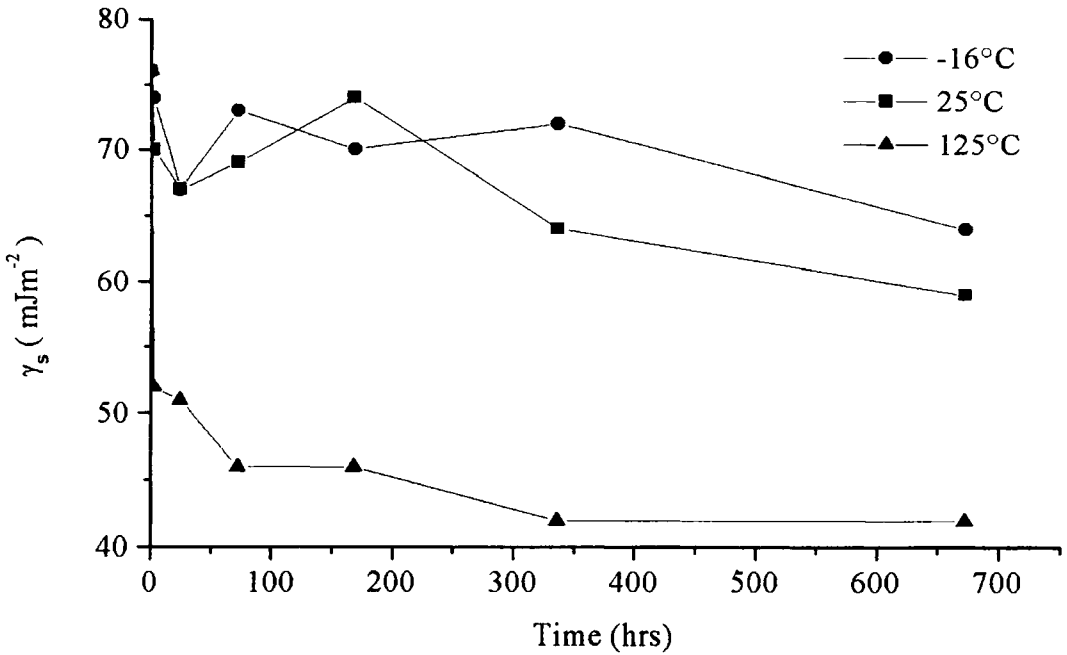

FIGURE 4 Effect of storage time after treatment and temperature on surface energy values of argon plasma treated GFR.PPS.

power of 100 W for argon and oxygen, respectively. Both treatments show a trend similar to the plasma treated GFR-PPS specimens. The water contact angle decreased immediately after treatment to a very low level for both argon and oxygen treated samples, and remained relatively stable when stored at minus 16°C. However, when stored at the higher temperatures these values increased with increase in storage time as shown in Tables III and IV. The contact angle values increased at a faster rate for samples stored at higher temperatures. This may be due to the fact that the oxide layer is forming at a faster rate at the higher temperature.

Surface Energy

Using Equations (1–4) and corresponding water and methylene iodide contact angles surface energy values were calculated. After argon plasma treatment of GFR-PPS the polar component of the surface energy increased to 34 mJm^{-2} from 7 mJm^{-2} for untreated GFR-PPS. However, this decreased after two hours and stabilized at 29, 22 and 9 mJm^{-2} for samples stored at −16°C, 25°C and 125°C, respectively. After the initial instability, values remained stable up to a month after treatment. The polar component of the samples stored at 125°C reduced to that of untreated GFR-PPS only two hours after treatment. The dispersive component was influenced only slightly by the treatment. Initially a value of 34 mJm^{-2} was determined. This increased to about 46 mJm^{-2} after treatment, which then stabilized in the low forties before dropping to about 37 mJm^{-2} one month after treatment. It was not affected to any great extent by storage temperature and only slightly by time.

For the oxygen treatment the polar component changed from an initial value of 7 mJm^{-2} to 38 mJm^{-2} after treatment. This was again stable at the lower temperatures but decreased to 19 mJm^{-2} after 2 hours storage at 125°C. The dispersive component increased even less than that of the argon treatment, from 34 mJm^{-2} before treatment to 36 mJm^{-2} after treatment. This was again stable up to one month after treatment.

These results are further highlighted in the total surface energy (γ_s) values, where the surface energy of the oxygen plasma treated GFR-PPS increased dramatically after treatment, decreased slightly

and then stabilised at 64 mJm^{-2} when stored at −16°C and 25°C as shown in Figure 5. This is not as clear for the argon plasma treated GFR-PPS specimens but at −16°C and 25°C the surface energy has not fallen below 60 mJm^{-2} after 30 days. The surface energy results for the plasma treated titanium are shown in Figs. 6 and 7. The surface energy remains relatively stable at −16°C but, as the temperature is increased, the values begin to decrease with increase in storage time.

Surface Morphology

Scanning Electron Microscopy (SEM)

As stated previously, the surface roughness was examined visually using SEM and quantitatively using AFM. Results for the GFR-PPS shown in Figures 8–10 illustrate the fact that the plasma treatments removed some of the matrix material and slightly exposed some of the fibres. The oxygen treatment looks more severe than the argon treatment in this respect. At higher magnification (Figure 11, untreated) the effect of the inert argon plasma (Figure 12) and the reactive oxygen (Figure 13) can be seen in more detail. By comparing these treated surfaces with the untreated ones, it can be seen that the argon treatment ablated away matrix material. The oxygen treatment, however, severely micro-etched the surface leaving a uniform cratered surface. This is further highlighted at higher magnifications for the GFR-PPS in Figures 14 and 15.

Atomic Force Microscopy (AFM)

There is further evidence of an increase in surface roughness for plasma treated GFR-PPS in the AFM results. The R_a values (Figures 16, 17 and 18) echo the results seen in the SEM images. Both treatments show an increase in surface roughness compared with untreated material. However, the oxygen plasma treatment produces a greater increase surface roughness with R_a values of 0.074 μm and 0. 141 μm recorded for argon and oxygen treatments, respectively, compared with 0.044 μm for the untreated surface.

The AFM results (Figures 19–21) show that plasma treatment also increases the micro-roughness of titanium. Again, the oxygen

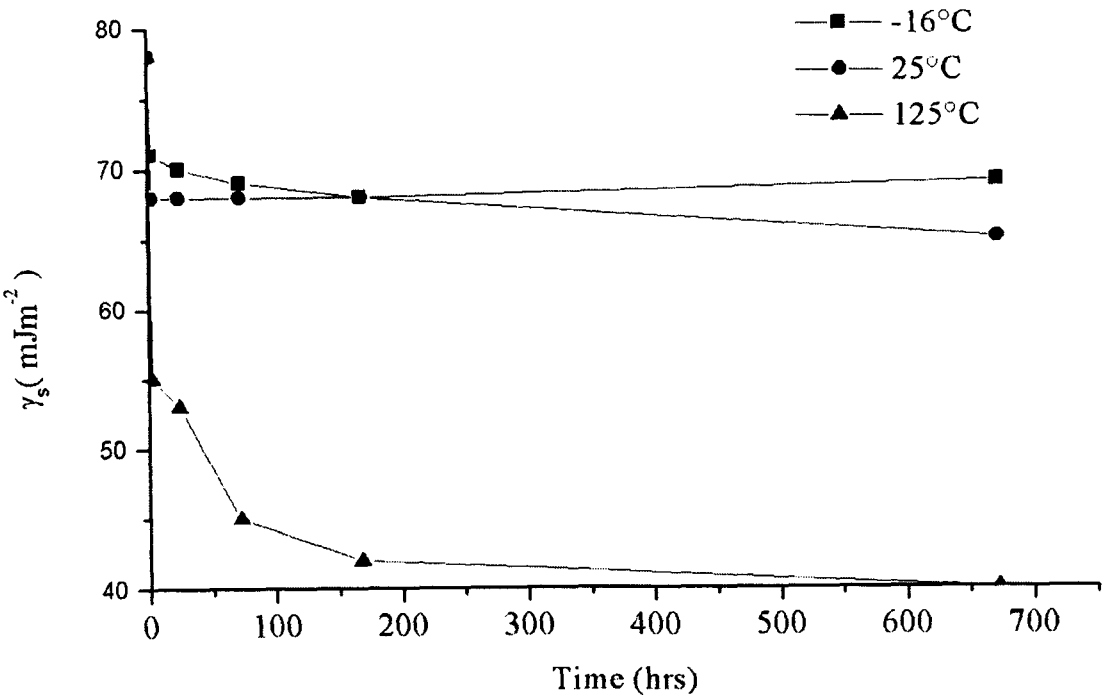

FIGURE 5 Effect of storage time after treatment and temperature on surface energy values of oxygen plasma treated GFR-PPS.

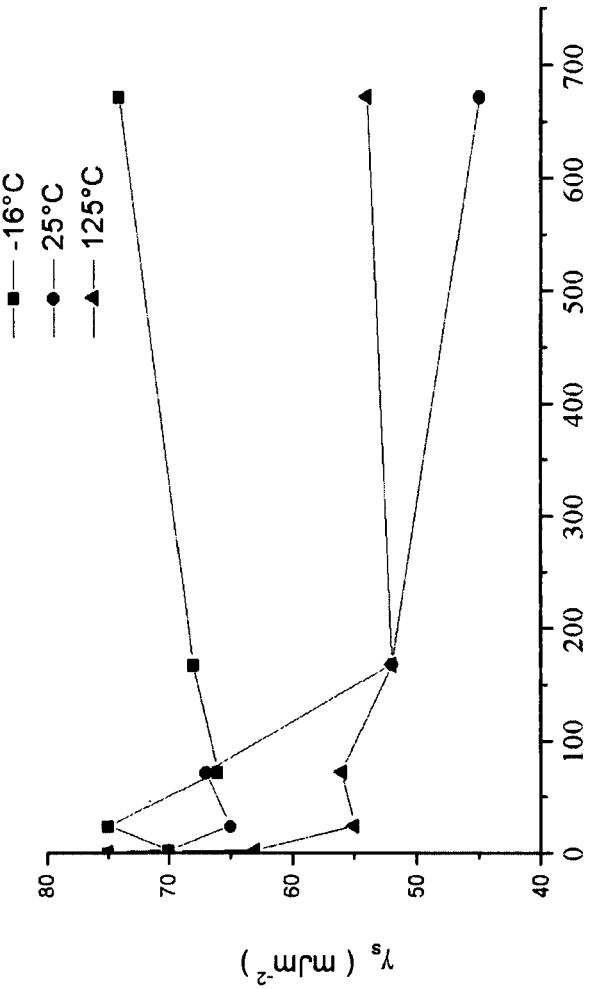

FIGURE 6 Effect of storage time after treatment and temperature on surface energy values of argon plasma treated titanium.

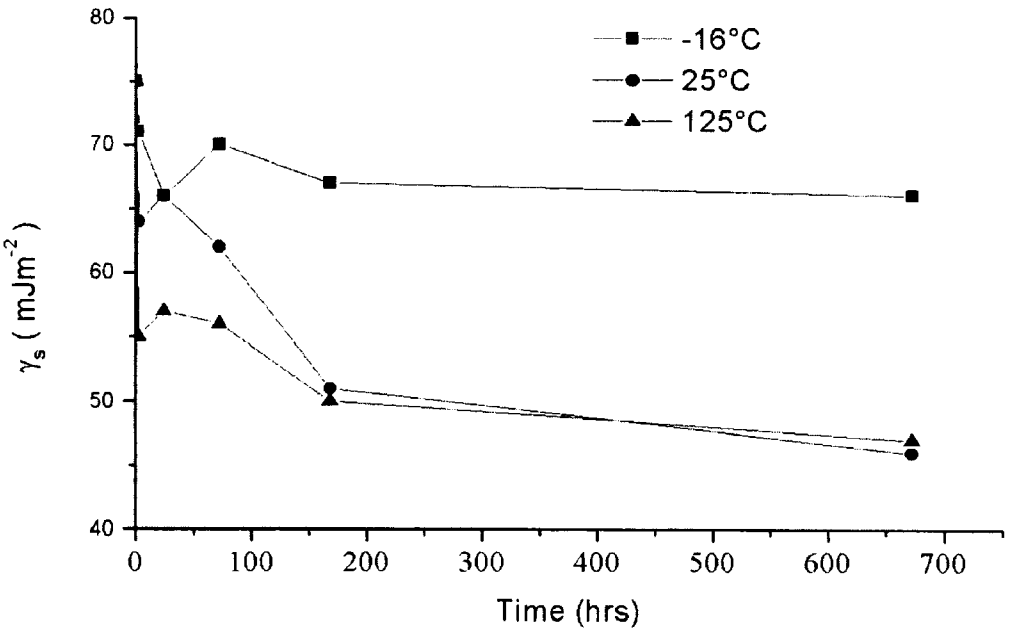

FIGURE 7 Effect of storage time after treatment and temperature on surface energy values of argon plasma treated titanium.

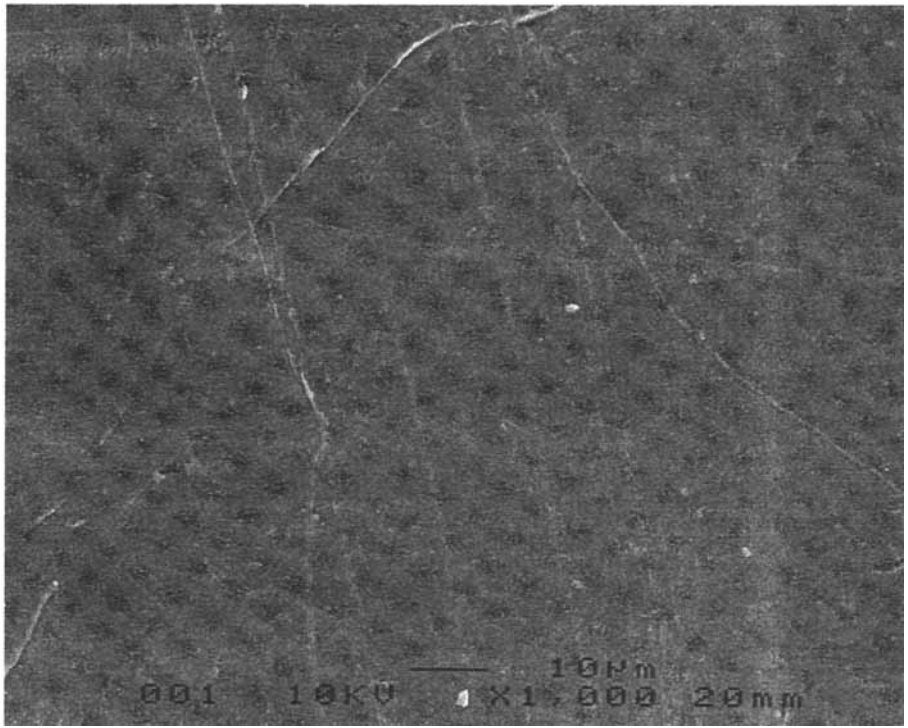

FIGURE 8 Untreated GFR.PPS (X1000).

FIGURE 9 Argon plasma treated GFR-PPS (XI000).

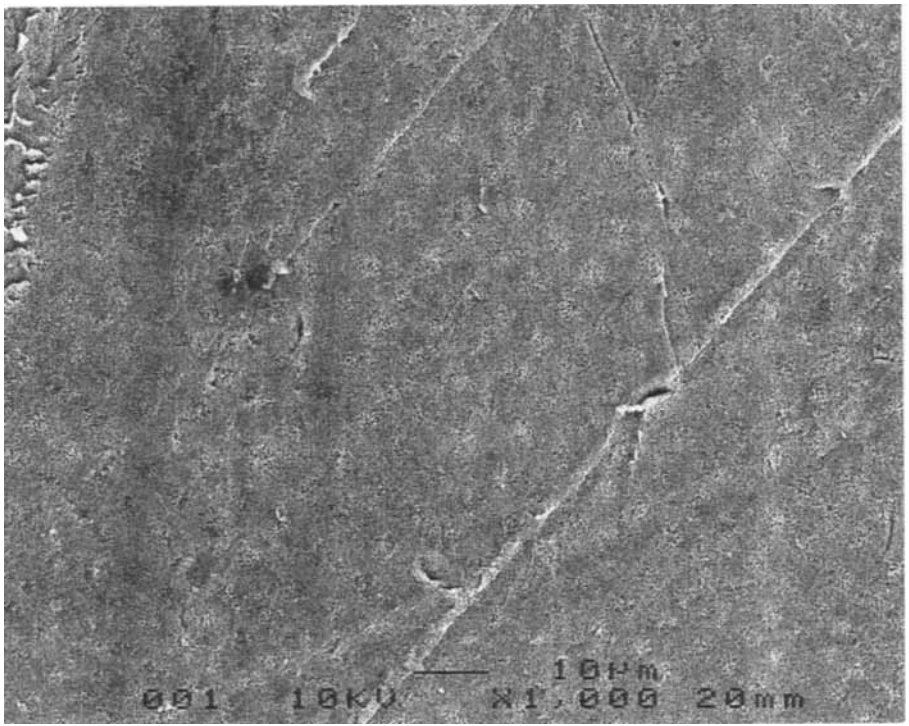

FIGURE 10 Oxygen plasma treated GFR-PPS (XI000).

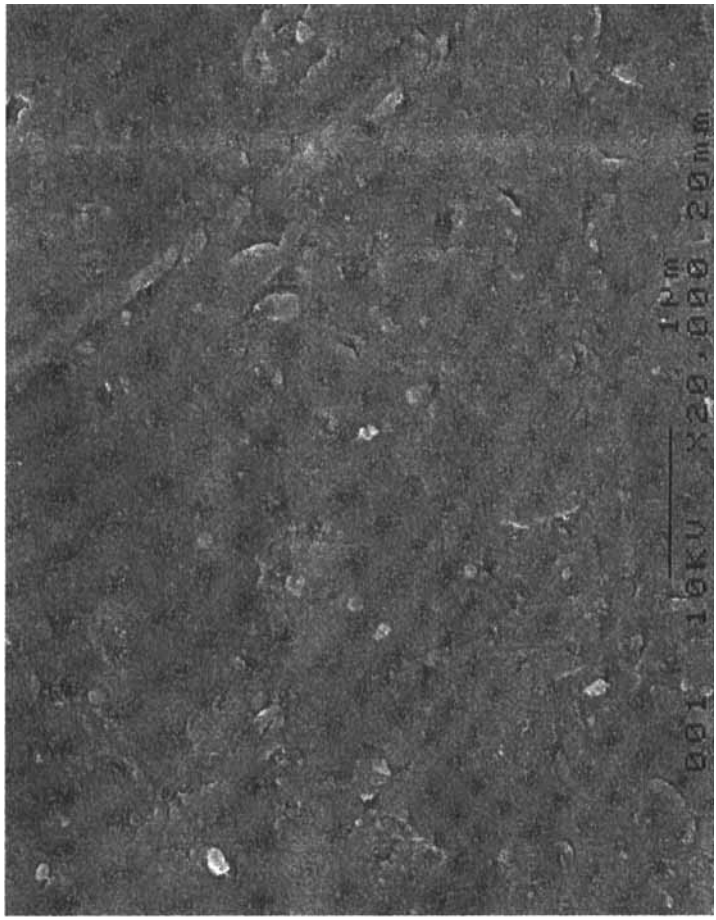

FIGURE 11 Untreated GFR-PPS (X20,0000).

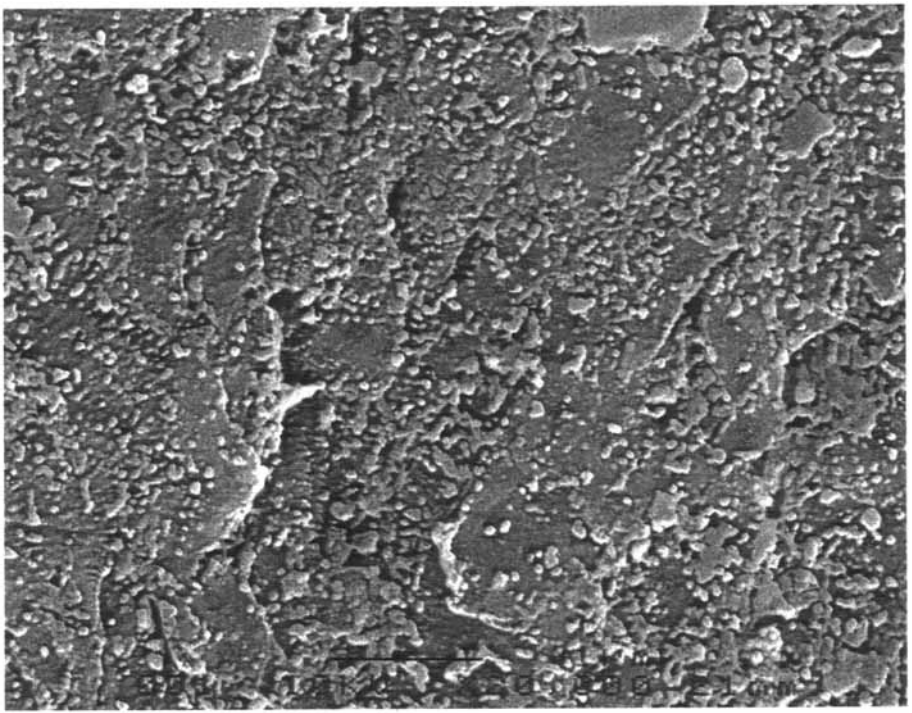

FIGURE 12 Argon plasma treated GFR-PPS (X20,000).

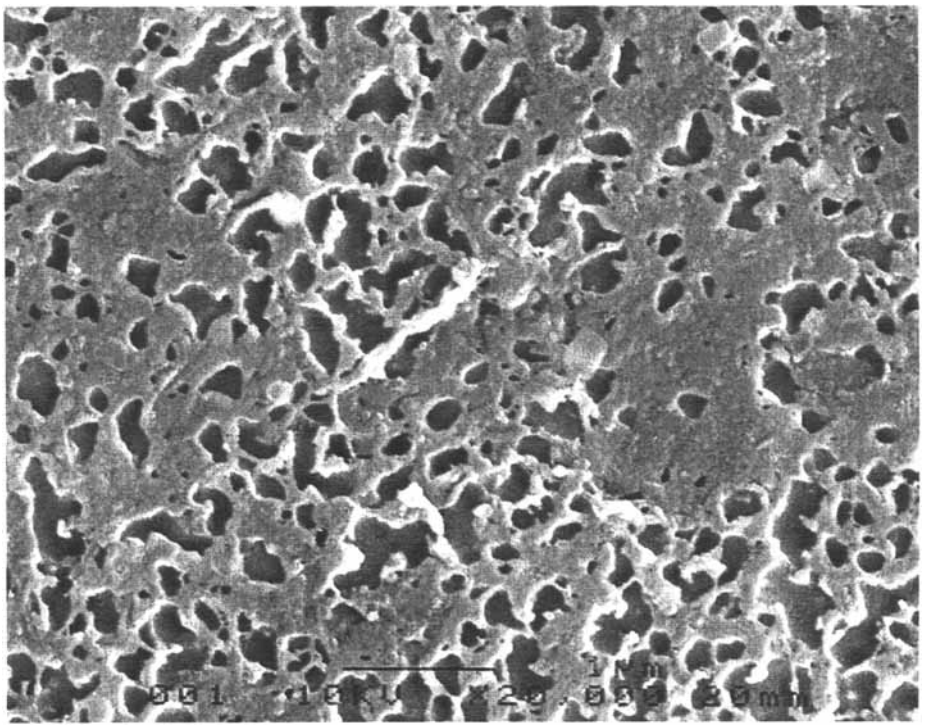

FIGURE 13 Oxygen plasma treated GFR-PPS (X20,000).

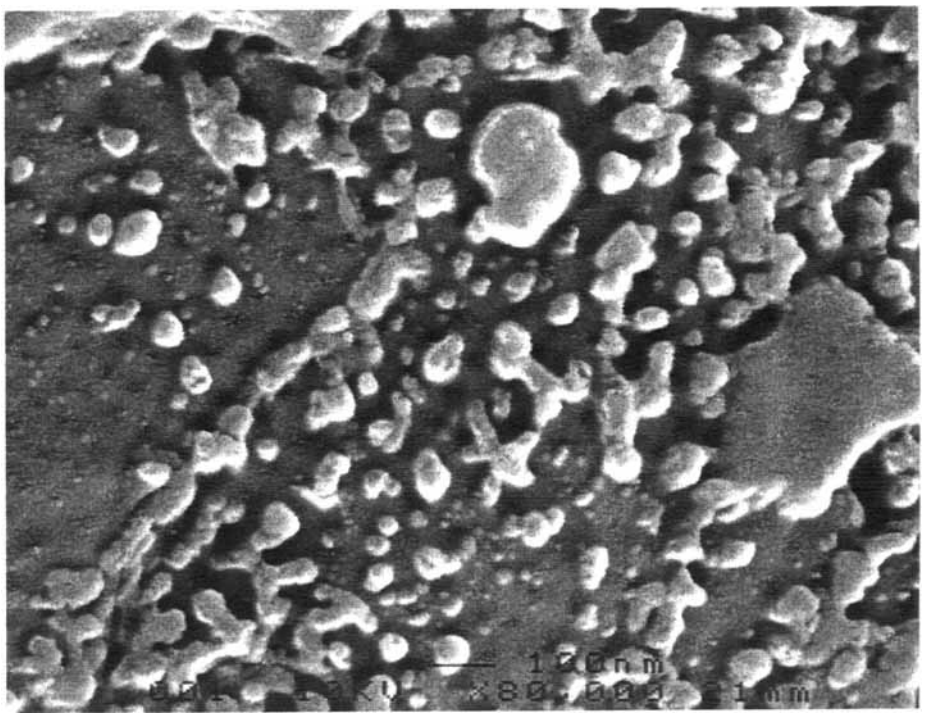

FIGURE 14 Argon plasma treated GFR-PPS (X80,000).

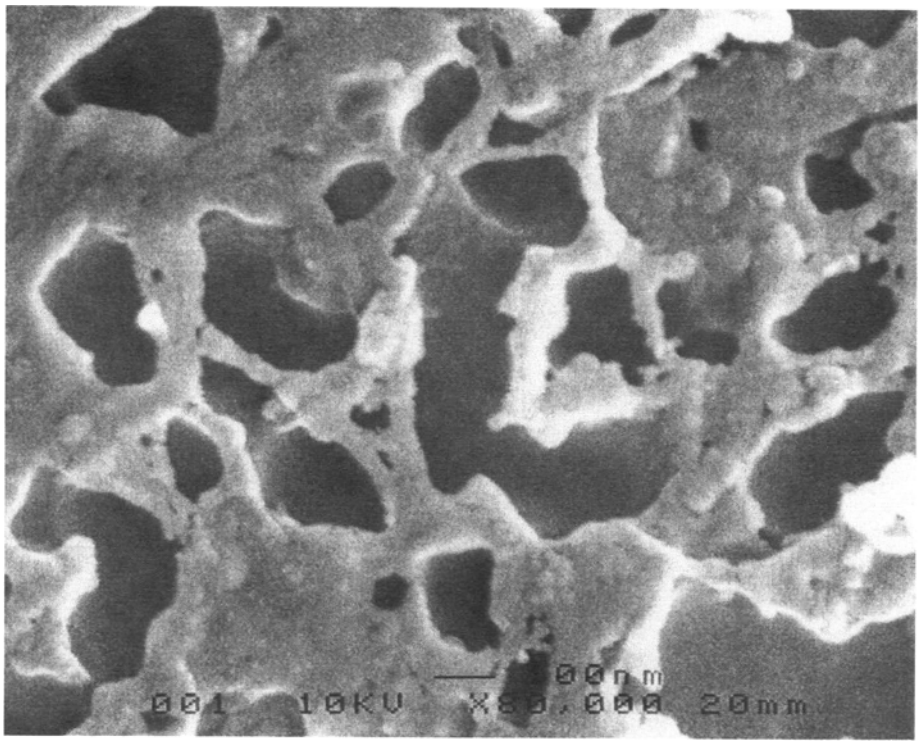

FIGURE 15 Oxygen plasma treated GFR-PPS (X80,000).

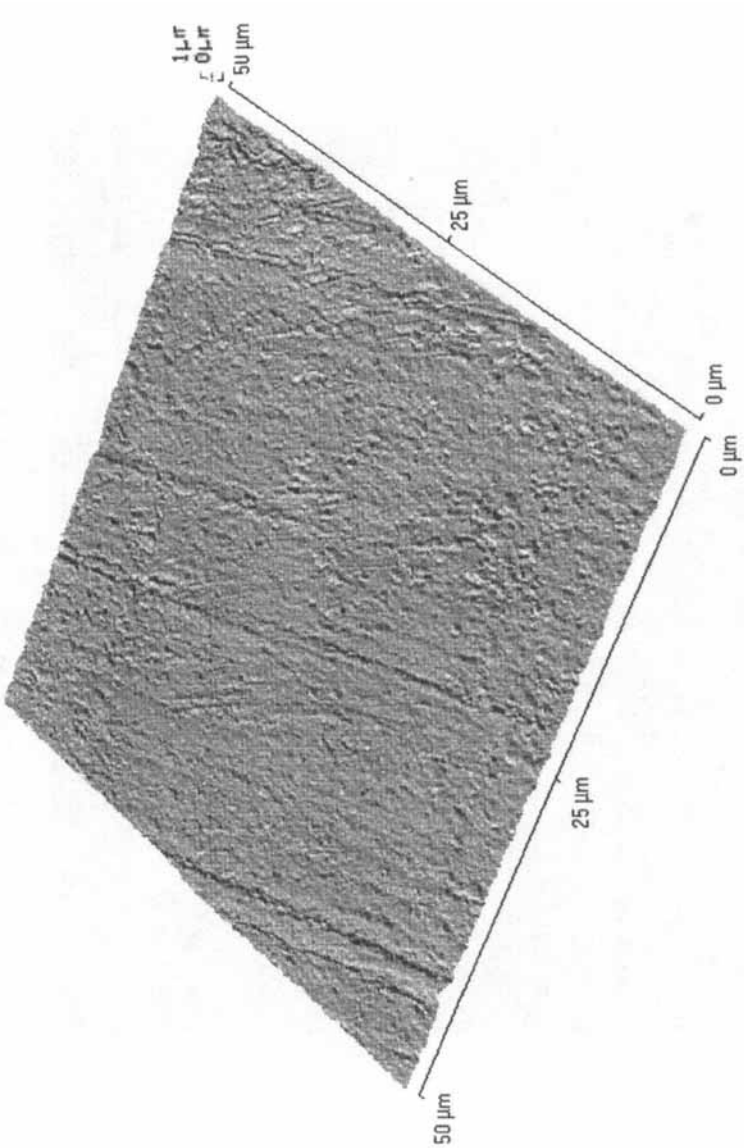

FIGURE 16 AFM image of untreated GFR-PPS ($R_a = 0.044$ µm).

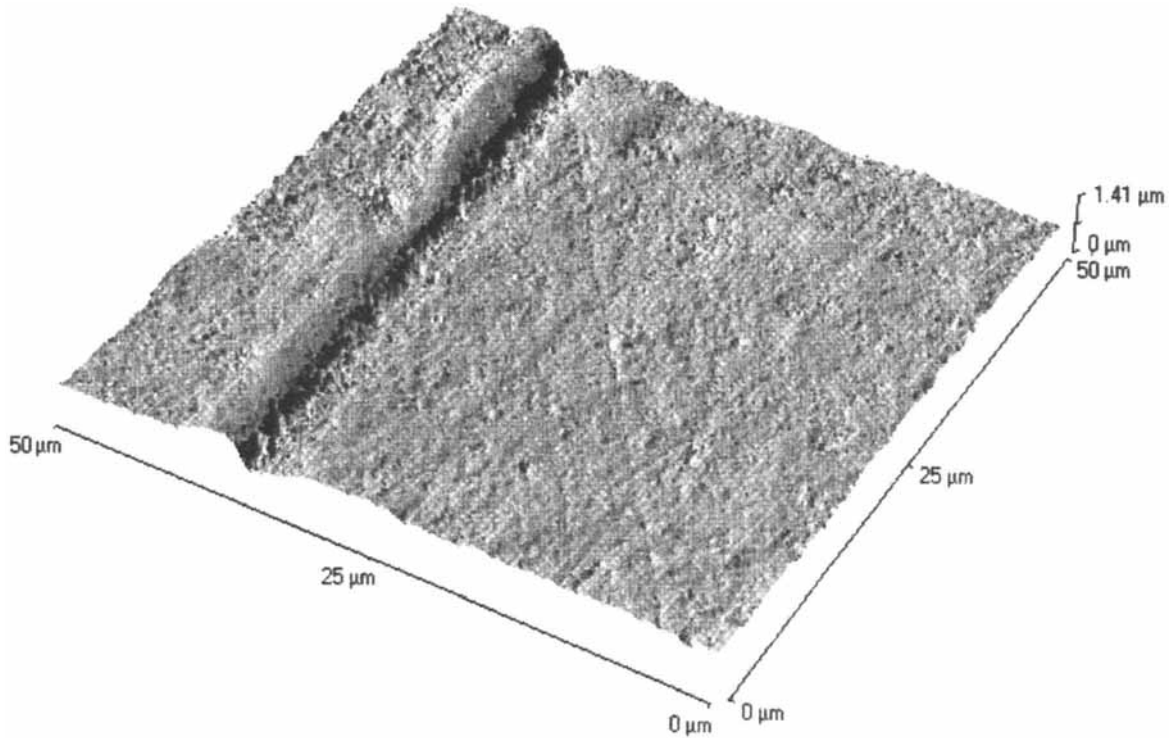

FIGURE 17 AFM image of argon plasma treated GFR-PPS ($R_a = 0.074\,\mu m$).

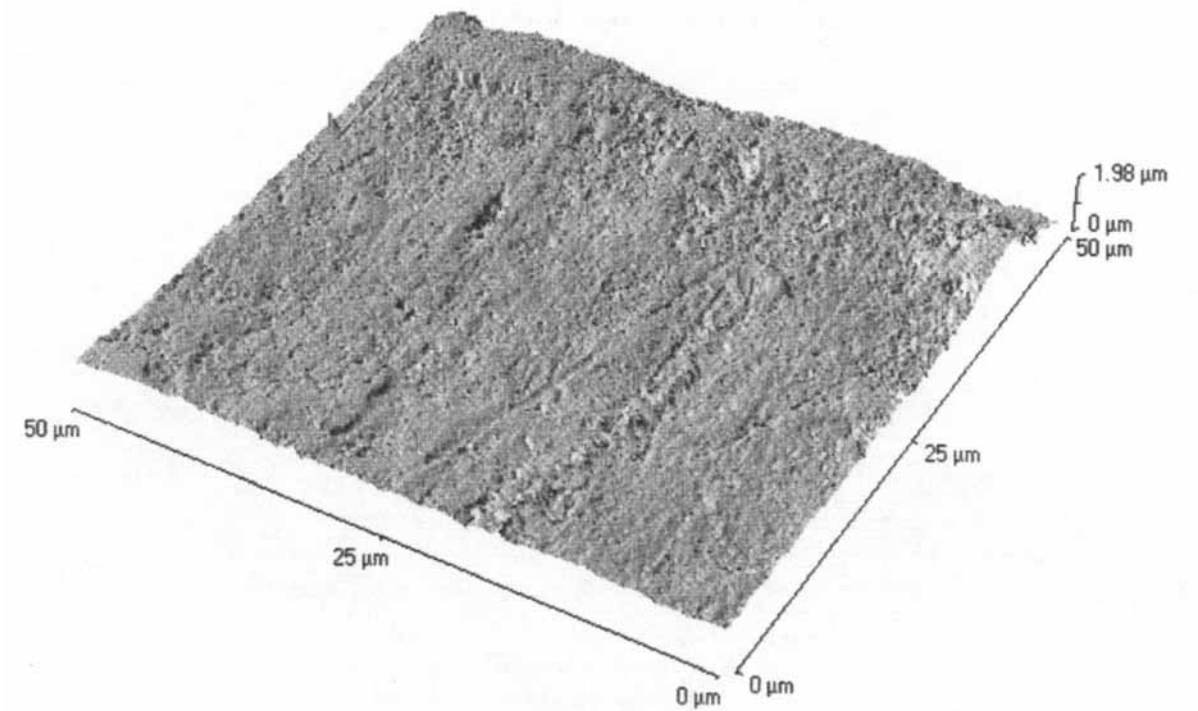

FIGURE 18 AFM image of oxygen plasma treated GFR-PPS ($R_a = 0.141\ \mu m$).

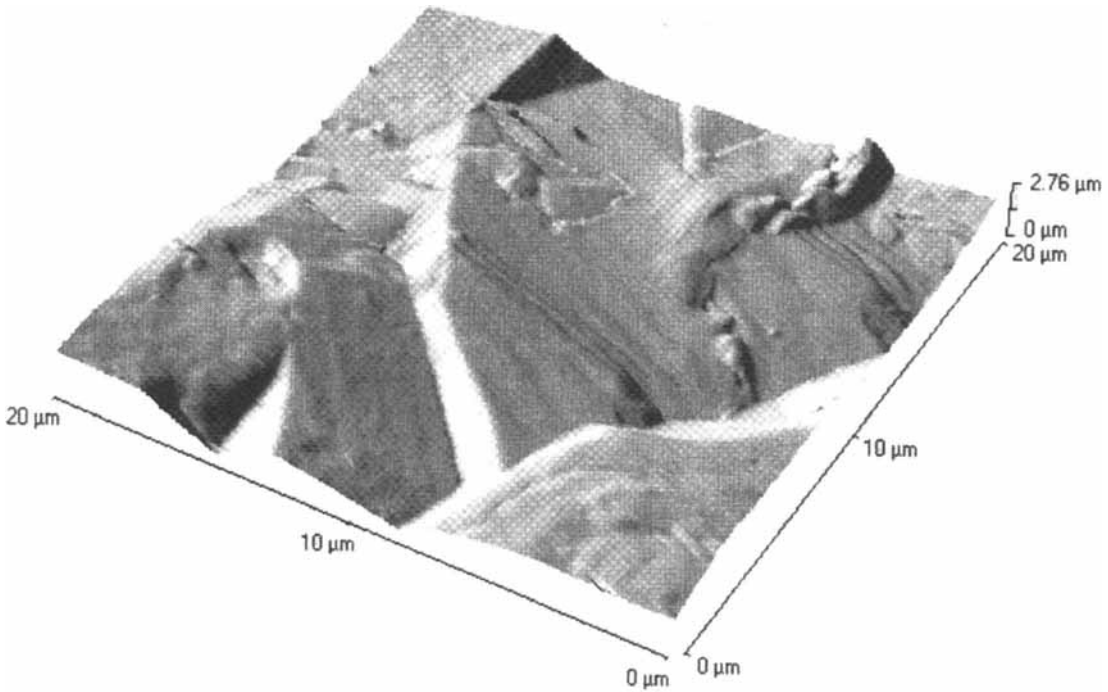

FIGURE 19 AFM image of untreated titanium ($R_a = 0.324\,\mu m$).

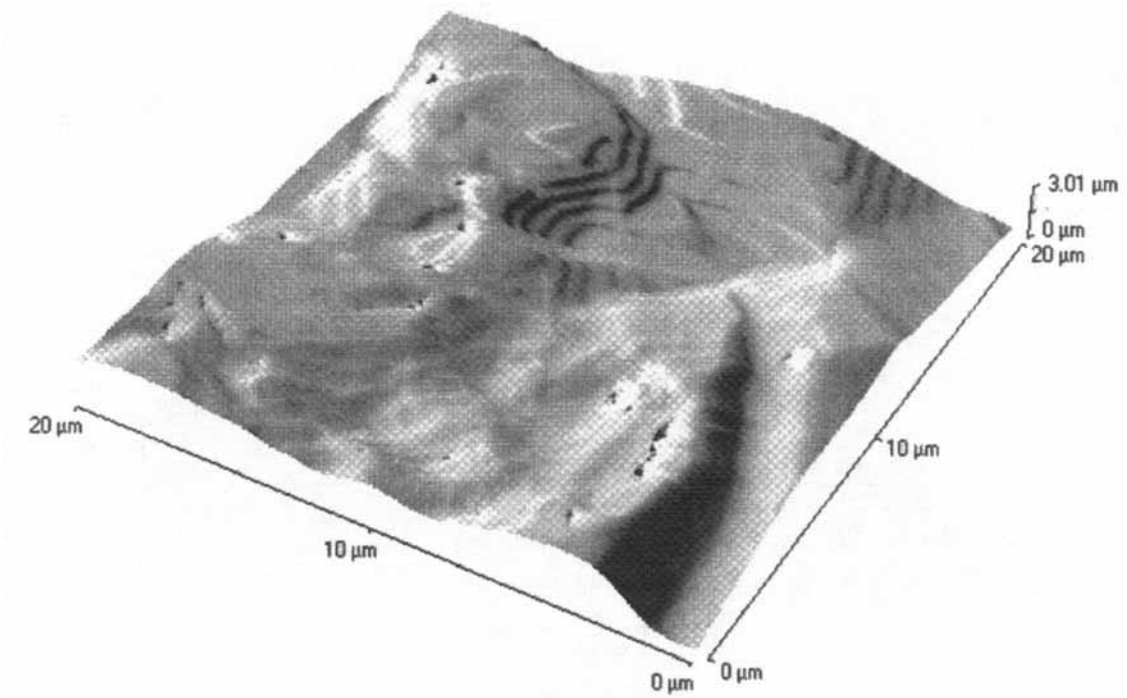

FIGURE 20 AFM image of argon plasma treated titanium ($R_a = 0.522\,\mu m$).

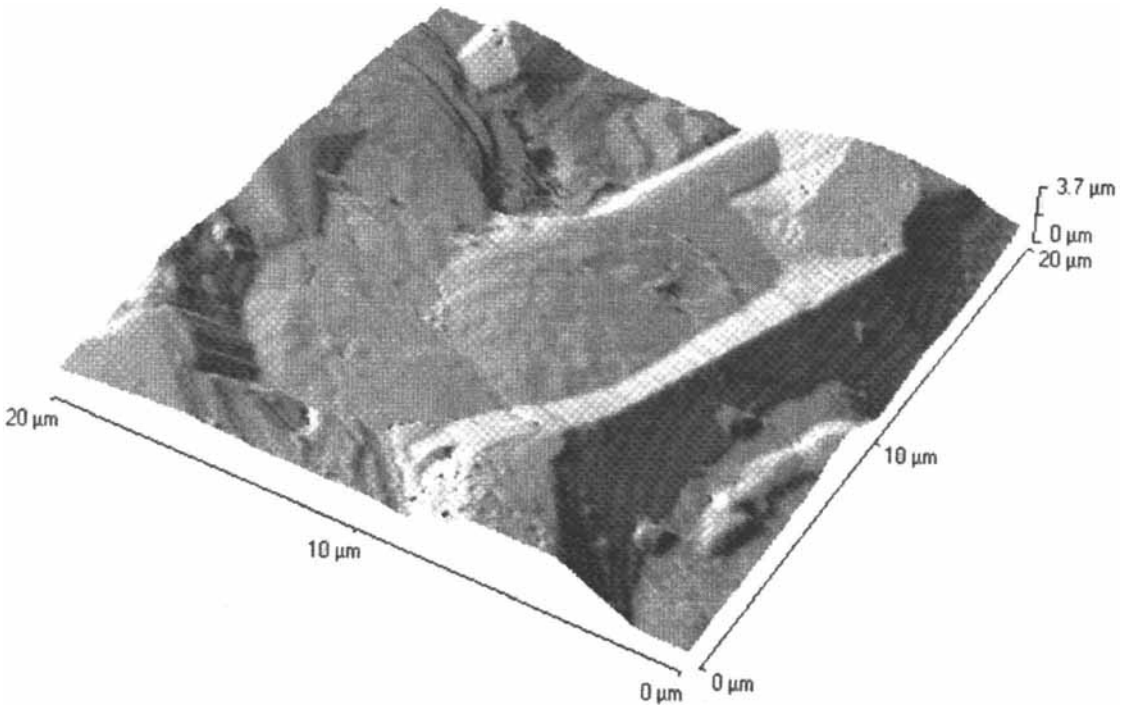

FIGURE 21 AFM image of oxygen plasma treated titanium ($R_a = 0.721$ µm).

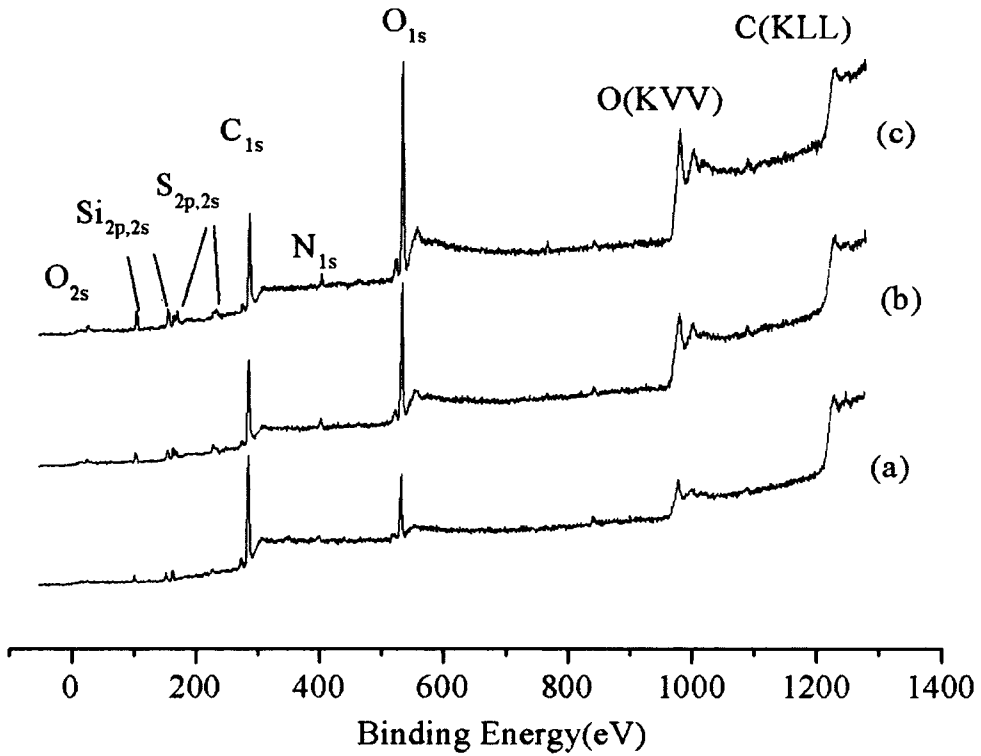

FIGURE 22 XPS analysis of untreated (a) argon plasma treated (b) and oxygen plasma treated (c) GFR-PPS.

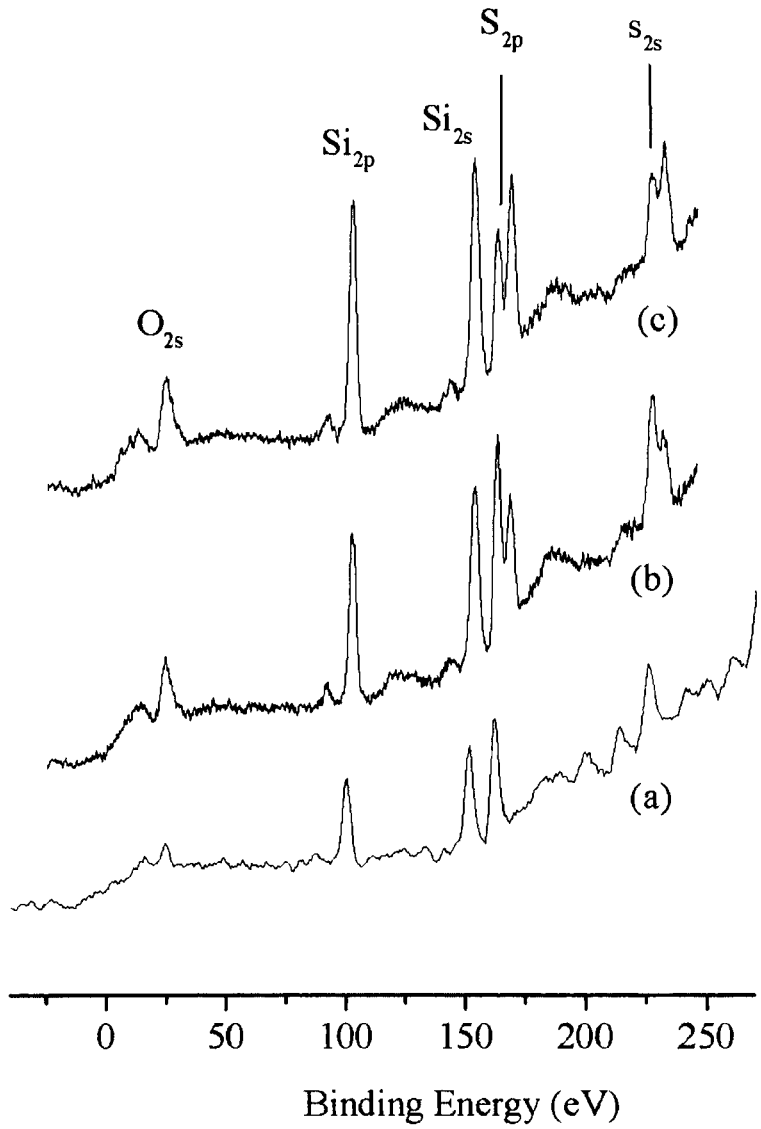

FIGURE 23 High resolution XPS analysis of untreated (a) argon plasma treated (b) and oxygen plasma treated (c) GFR-PPS.

treatment resulted in the greatest increase in R_a, with values for untreated, argon-treated and oxygen-treated titanium of 0.324 μm, 0.522 μm and 0.721 μim, respectively.

Surface Chemistry Analysis

X-ray photoelectron spectroscopy analysis of the plasma treated surfaces reveal changes in the surface chemistry of the specimens as a result of plasma treatment. The peaks of interest in the spectra of the GFR-PPS samples are C_{1s}, O_{1s}, O_{2s}, S_{2s}, S_{2p}, Si_{2s}, Si_{2p} and N_{1s}. Firstly, it is shown in Figure 22 that the oxygen Content ($\sim$ 530 eV) has increased for the argon-treated sample and even more so for the oxygen-treated sample. The O:C ratio increases from 1:0.7 for the untreated surface to 1:2 and 1:3 for the argon and oxygen plasma treated surfaces, respectively. These changes may be due an increase in the concentration of carbon-oxygen (C-O) groups and the introduction of carbonyl (C=O) and carboxylic acid (O-C=O) groups [1] on the surface of the plasma-treated specimens.

The S_{2s}, S_{2p} peaks in Figure 23 are also of interest, with a shift of approximately 5 eV in binding energy. The higher binding energy peak may be due to surface sulphur-oxygen (S=O) groups. The surface spectrum of the oxygen-treated sample also reveals that the Si peaks are shifted by $\sim$ 1.2 eV upwards in binding energy from the untreated GFR-PPS surface. This is consistent with the etching of

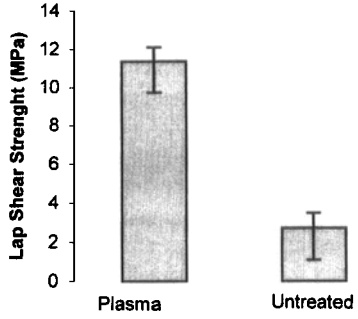

FIGURE 24 Lap shear strengh of GFR-PPS/Titanium adhesive bonds.

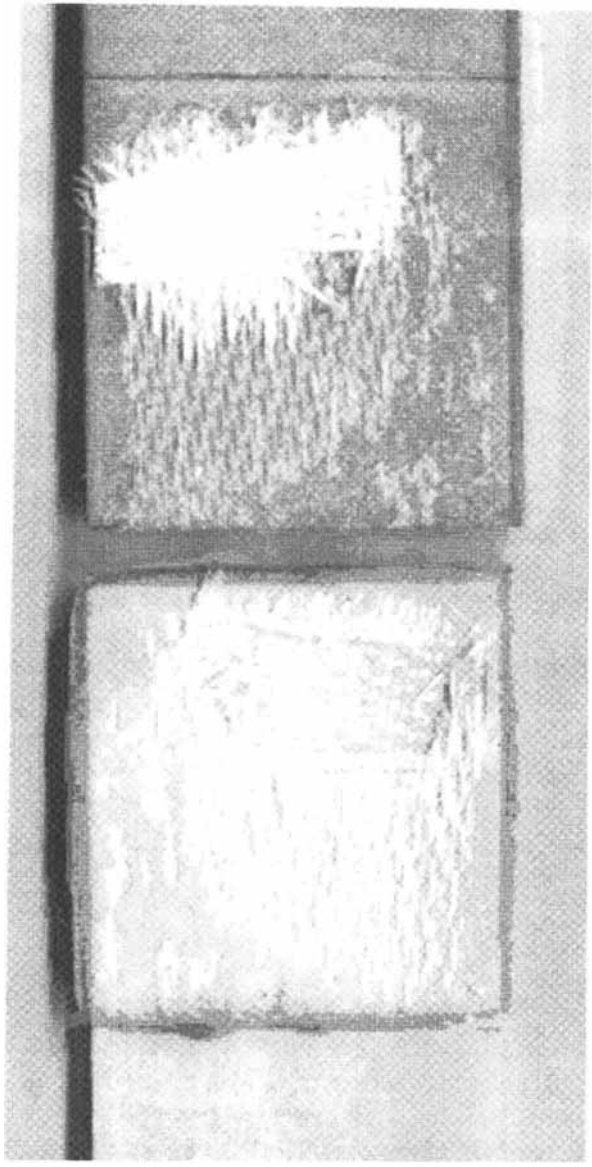

FIGURE 25 Evidence of delamination of composite after lap shear testing.

the matrix surface seen in the SEMs, Figures 8–10. More of the matrix material seems to have been etched away on the oxygen-treated surface, thereby exposing and oxidising some glass fibres. As a result, the Si_{2s}, and Si_{2p} peaks are more intense for the oxygen treatment. From Figure 22 it is also evident that we have an increase in nitrogen content of the surfaces. Similar behaviour is observed for the argon plasma treated surface but with one interesting difference; the new S_{2s}, and S_{2p} peaks are less intense than those observed for the oxygen-treated GFR-PPS surface. The increase in oxygen content for the argon plasma treated surface is probably due to residual radicals reacting with air after exposure to the atmosphere but the possibility of residual air in the chamber during treatment cannot be ruled out.

Bond Strength Evaluation

As the oxygen treatment exhibited the most stable contact angles and showed the greatest increase in roughness for both titanium and GFR-PPS it was chosen as the preferred method for bonding and mechanical strength evaluation. As discussed previously, the bond strength was determined by lap shear testing according to ASTM standard D 5868-95. The results shown in Figure 24 show an increase in bond strength of over 7 MPa for oxygen plasma treated specimens with a value of 11.3 MPa recorded, compared with 2.9 Mpa for the degreased specimens.

Failure of the untreated joints occurred at the GFR-PPS/Adhesive interface, while the plasma-treated adhesive joints failed due to delamination of the composite material as seen in Figure 25.

CONCLUSIONS

Plasma treatment is an effective method of surface treatment for both GFR-PPS and titanium. The optimum parameters for argon and oxygen plasma treatments were determined to be 100 W, 40 Pa operating pressure for 30 minutes and 100 W, 40 Pa operating pressure for 10 minutes, respectively. Surface chemistry analysis has shown that both plasma treatments results in an increase in the oxygen content of

the surface regions. However, oxygen plasma treatment resulted in the greatest increase in surface energy, O:C ratio and surface roughness for both GFR-PPS and titanium, hence, it was chosen as the preferred method of surface treatment prior to bonding. Lap shear tests have revealed a significant increase in bond strength with values increasing from 2.9 MPa for untreated surfaces to 11.3 MPa for oxygen plasma treated surfaces.

References

[1] Blackman, B. R. K., Kinloch, A. J. and Watts, J. F., *Composites* **25**(5), 332 (1994).
[2] Comyn, J., Mascia, L., Xiao, G. and Parker, B. M., *Int. J. Adhes. & Adhes.*, **16**(2), 97 (1996).
[3] Kinloch, A. J., *Adhesion and Adhesives* (Chapman and Hall, London, 1987), Chap. 4, pp. 129, 159.
[4] Ameen, A. P., *Polymer Degradation and Stability* **51**, 179 (1996).
[5] Barron, V. and Schue, F., *Int. J. Adhes. & Adhes.* **20**(5), 361 (2000).
[6] Brennan, W. J., Feast, W. J., Munro, H. S. and Walker, S.A., *Polymer* **32**(8), 1527 (1991).
[7] Chatelier, R. C., Xie, X. M., Gengenbach, T. R. and Gresser, H., *J. Langmuir* **11**(7), 2576 (1995).
[8] Strobel, J. M., Strobel, M., Lyons, C. S., Dunatov, C. and Perron, S. J., *J. Adhesion Sci. Technol.* **5**(2) (1991).
[9] Nakamatsu, J., Delgado-Aparicio, L. F., Da Silva, R. and Soberon, F., *J. Adhesion Sci. Technol.* **13**(7), 753 (1999).
[10] Renegar, T. S., *Modern Plastics Encyclopaedia'91*, (McGraw-Hill, New York, 1990), Chap. 1, p. 83.
[11] Kohli, D., *Int. J. Adhes. & Adhes.* **19**(2–3), 231–242 (1999).
[12] Foerch, R., Kill, G. and Walzak, M. J., *J. Adhesion Sci. Technol.* **17**, 1077 (1993).